



Photooxidation of particulate organic matter, carbon/oxygen stoichiometry, and related photoreactions

Margaret L. Estapa*, Lawrence M. Mayer

School of Marine Sciences, University of Maine, Darling Marine Center, 193 Clark's Cove Rd., Walpole, ME 04573, United States

ARTICLE INFO

Article history:

Received 30 December 2009
Received in revised form 29 June 2010
Accepted 30 June 2010
Available online 4 July 2010

Keywords:

Photochemistry
Suspended particulate matter
Organic carbon
Oxidation
Photo-Fenton

ABSTRACT

We investigated photoredox transformations of oxygen, carbon, peroxides, and iron that accompany “photodissolution” of suspended marine particulate organic carbon (POC), a sunlight-induced process that transfers POC to the dissolved organic carbon (DOC) pool. During 18- to 24-hour photodissolution experiments with POC of varying composition, about 0.28 mol of O₂ was consumed per mole POC photodissolved. Mean dissolved inorganic carbon (DIC) production was 6% of initial POC in suspended river delta sediments and 1% in algal membrane detritus. The mean O₂ loss:DIC production ratio was –1.3:1 in sediment suspensions, which slightly exceeds the typical range reported for DOC. The O₂ loss:DIC production ratio was –7.7:1 in suspensions of algal detritus, which implies significant oxygen incorporation into (oxygenation of) organic matter. Irradiated sediment suspensions rapidly achieved low, steady-state peroxide concentrations but rose more slowly with algal detritus. Elevated iron concentrations in the 0.7–8.0 μm particle size fraction after 24 h of irradiation are consistent with photoredox cycling of metals and/or with physical disintegration of organic-mineral aggregates driven by organic matter dissolution. These oxidation and oxygenation results differ from analogous reactions previously found for marine DOC, and estimates of DIC production in particle-rich environments will require incorporation of POC-specific information.

© 2010 Elsevier B.V. All rights reserved.

1. Introduction

Over the last several decades, sunlight's role in DOC transformations in marine and aquatic environments has been extensively investigated (Mopper and Kieber, 2002). In recent years, researchers have shown that POC is also susceptible to photochemical alteration, as might be expected from its high local concentrations of pigments, transition metals, and other particle-associated organic components (Zafriou, 2002). The operationally-defined transformation of POC to DOC, termed “photodissolution” by Mayer et al. (2006), has been documented in sediments from a shallow, subtropical river delta (Mayer et al., 2006), across a turbid estuarine gradient (Kieber et al., 2006), in freshwater river sediments (Riggsbee et al., 2008), and in cellular detritus of cultured algae (Mayer et al., 2009b). These are all examples or analogs of high-POC aquatic and marine systems where particulate matter can make up a significant fraction of photochemically-reactive material in the sunlit layer. The photodegradation reactions of phytoplanktonic lipids, reviewed by Rontani (2001), have been suggested as tracers of these particle-hosted photochemical reactions.

The oxidative nature of organic matter photodegradation is well-established. Dissolved inorganic carbon (DIC) is the primary identifiable photoproduct (Miller and Zepp, 1995), followed by carbon monoxide at about 1/20th the concentration of DIC (Miller and Zepp, 1995; Gao and Zepp, 1998). Xie and Zafriou (2009) recently demonstrated that CO photoproduction by particles isolated from blue-water and coastal environments is at least as efficient as CO photoproduction by DOC. Xie et al. (2004) demonstrated that oxygen drives photoproduction of DIC from DOC in river water. Photoproduction of DIC from POC has not yet been demonstrated, but Mayer et al. (2006,2009b) reported organic carbon budget shortfalls of several percent during photodissolution that are consistent with DIC photoproduction.

Various reactive oxygen species form during DOC photodegradation, with possible broad effects on carbon, oxygen, and trace metal cycling (Blough and Zepp, 1995). Hydrogen peroxide, the most persistent of these species, accumulates in natural waters (Cooper et al., 1988; Andrews et al., 2000; O'Sullivan et al., 2005), and photochemical oxygen consumption is common (Miles and Brezonik, 1981; Amon and Benner, 1996; Gao and Zepp, 1998; Andrews et al., 2000; Obernosterer et al., 2001; Xie et al., 2004). Andrews et al. (2000) tabulated ratios of O₂ and H₂O₂ quantum yields to examine relationships among photochemical oxygen consumption, DOC oxidation, and H₂O₂ production. They postulated a net ratio of 1.1 mol O₂ lost per mole CO₂ produced from DOC photooxidation, and

* Corresponding author. Tel.: +1 207 563 3146x220; fax: +1 207 563 3119.
E-mail address: margaret.estapa@maine.edu (M.L. Estapa).

a mean 3-electron oxidation of DOC per O₂ consumed. They found that 45% of gross O₂ consumption was likely due to formation of H₂O₂, which in natural waters decomposes mainly back to O₂ and H₂O (Andrews et al., 2000).

Several authors have postulated that photochemically-produced H₂O₂ and Fe(II) react to produce hydroxyl radicals (“photo-Fenton” chemistry), and contribute to photodegradation of DOC in fresh- or coastal waters with high Fe concentrations and low pH (Moffett and Zafriou, 1993; Miller et al., 1995; Southworth and Voelker, 2003). The data of Moffett and Zafriou (1993) suggested that in the Orinoco River plume, the photo-Fenton reaction depended specifically on particulate Fe, although most reports describe the involvement of colloidal or transient dissolved Fe(II).

Thus coastal and aquatic DOC undergoes photochemically-driven redox transformations of organic carbon, oxygen, and transition metals. Here we explore similar processes and impacts for POC. Using the extensive literature regarding DOC photooxidation to develop metrics for comparison, we present an experimental survey of the major photoprocesses—i.e., DIC production, peroxide cycling, O₂ loss, and Fe cycling—expected to affect two contrasting types of POC.

2. Methods and materials

2.1. POC suspensions

We used a nearshore sediment from the littoral zone near Freshwater Bayou, Louisiana, a turbid, productive, shallow region west of the Atchafalaya River delta (see “FWB” site description in Mayer et al., 2009a). Sediments were freeze-dried and then gently ground to pass a 63 μm sieve prior to use. Sediments contained 1.98% organic carbon and 2.00% total carbon by weight (see below). The sample had a starting C:N ratio of 8.7, a δ¹³C value of −22.8‰, a total lignin (A₈) content of 1.55%, and a ¹⁴C modern fraction of 0.8970 (Mayer et al., 2009a). Pigment content data were not available for this sample, but typically range 1–20 μg-chlorophyll g-dry weight^{−1} in the study area. In this region, suspended riverine and coastal sediments typically contain 2–5% iron by weight (e.g., Horowitz et al., 2001; Swarzenski et al., 2006).

Sediments were resuspended at a concentration of 500 mg L^{−1} in low-OC artificial seawater with carbonate salts omitted, to give suspension concentrations of ~830 μM POC and 9.6 μM particulate inorganic carbon (PIC). This concentration was chosen to ensure measureable changes in carbon pools and represent typical shallow-water conditions in coastal Louisiana at the peak of wind-driven resuspension events (e.g., Perez et al., 2000). To study the reactivity of POC of recent biological origin, algal membranes (*Tetraselmis* sp., Strain 429; Reed Mariculture, Campbell, CA) were isolated by centrifugation, after ultrasonication to remove cytoplasmic DOC, and freeze-dried and stored dry and frozen. This sample had a C:N ratio of 6.2, a chlorophyll content of approximately 16.2 mg g-dry weight^{−1} and a phaeopigment content of approximately 8.0 mg g-dry weight^{−1} (Mayer et al., 2009b). Algal membranes were resuspended in artificial seawater at concentrations of 50 or 100 mg L^{−1} (~1600 or 3200 μM POC), chosen to correspond to previous work (Mayer et al., 2009b). Artificial seawater used in suspensions to be tested for O₂ consumption was allowed to equilibrate with the lab air overnight, reaching ~210 μM O₂ at room temperature. In suspensions to be analyzed for DIC or peroxides, artificial seawater was made up and used immediately to minimize background peroxide formation and exchange with atmospheric CO₂. Suspensions were not sterilized or poisoned in order to avoid potential chemical artifacts from these treatments. Analysis of initial (t=0) suspensions and dark controls for all experiments allowed background levels of all analytes to be established before and after irradiation.

2.2. Irradiation experiments

Irradiations were conducted in an Atlas Suntest XPS Solar Simulator for continuous periods of 18 or 24 h. The xenon lamp was filtered to deliver output equivalent to subtropical, midday sunlight (Mayer et al., 2006). Suspensions were irradiated in two container configurations, both cooled in a water bath held at room temperature (20 °C ± 2 °C). Samples to be analyzed for DIC or O₂ were irradiated in headspace-free quartz tubes. Tubes were closed with silicone stoppers wrapped in precombusted aluminum foil to eliminate suspension contact with irradiated silicone (Lindell et al., 2000), and sealed outside the tube with Parafilm. Tubes were shaken by hand at intervals of 6–8 h to visually homogenize the suspension. Suspensions not requiring DIC or O₂ analysis were irradiated in glass beakers with quartz lids that were magnetically stirred with glass-encapsulated stir bars. All glassware was precombusted at 500 °C for at least 4 h. A side-by-side, 24 h irradiation of sediment suspensions in beakers and tubes showed that concentrations of POC and DOC measured in sediment suspensions before and after irradiation, and in non-irradiated controls, were not significantly different in tube and beaker configurations (Fig. 1). Simultaneous dark controls were conducted for every experiment, with tubes and/or beakers placed in the dark outside the solar simulator and kept at room temperature (20 ± 2 °C). Irradiated and dark control suspensions were subsampled in triplicate for all analyses just before the start of an irradiation (t=0) and at the end. Two replicate 48-hour experiments with sediments (one for OC and O₂, the other for peroxides) and one 24-hour experiment with algal POC (for peroxides) were conducted in order to investigate reaction kinetics; in these, suspensions were removed and analyzed at intervals throughout a 24-hour irradiation period and a subsequent dark 24-hour period.

2.3. Chemical measurements

POC samples were collected from suspensions by syringe filtration onto triplicate precombusted GF/F filters (ca. 0.7 μm pore size: Whatman) and stored frozen until analysis. For POC analysis, carbonates were removed from sediment samples by fuming the filters with HCl for 24 h (Mayer, 1994). Initial carbonate content of sediment was measured by difference from unacidified samples. Carbon and nitrogen were determined on a Perkin Elmer 2400B Elemental Analyzer calibrated against acetanilide standards. The POC detection limit, including sample handling, was 5 μM.

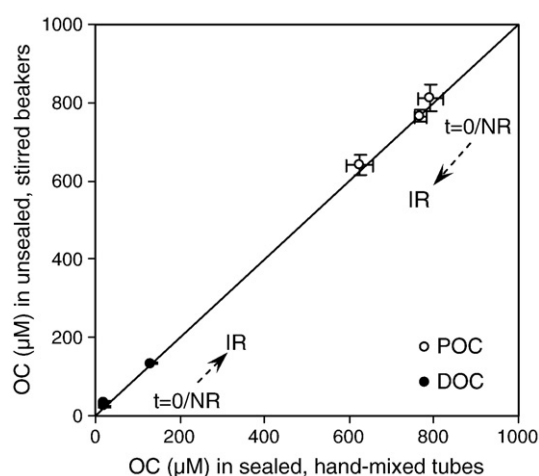


Fig. 1. POC (open circles) and DOC (filled circles) determined in sealed, headspace-free, hand-mixed tubes (x-axis) and in magnetically-stirred, unsealed beakers (y-axis). Error bars show one standard deviation (N=3 for POC; N=2 for DOC). Annotations and arrows on graph indicate initial and control suspensions, and direction of change in irradiated suspensions. The 1:1 line is shown for reference.

Filtrates from POC samples were collected for DOC analysis. Samples were stored frozen in precombusted glass vials until analysis, then acidified to pH 2 with 25% phosphoric acid to remove DIC. DOC content was determined using a Shimadzu TOC-V_{CPH} Total Organic Carbon Analyzer calibrated against standard solutions of potassium hydrogen phthalate. Samples were sparged with CO₂-free air, combusted over platinum catalyst, and the product CO₂ quantified with a non-dispersive infrared (NDIR) detector. The DOC detection limit was 7.5 μM.

Dissolved oxygen was determined via Winkler titrations (Carpenter, 1965). Triplicate tubes for oxygen analysis were fixed with manganese chloride and alkaline sodium iodide reagents immediately after removal from the solar simulator. Triplicate titrations with sodium thiosulfate standardized against potassium iodide were conducted by hand for each tube. The O₂ detection limit (calculated from reagent and sample blanks) was 14 μM and measurement precision was 5 μM.

DIC concentrations were determined from unfiltered aliquots of POC suspensions. Subsamples of about 10 mL were collected by pipetting from the middle of the irradiation tube or beaker, with care taken to avoid disturbing the air–water interface. Aliquots were immediately sealed with Parafilm and analyzed using the IC reactor of the Shimadzu TOC-V_{CPH}. Samples were acidified in-line with 25% phosphoric acid and sparged with CO₂-free air. Captured gases were analyzed via NDIR for CO₂. The detection limit for DIC by this method was 1.5 μM. Preliminary tests showed slightly higher concentrations of DIC in subsamples filtered through a GF/F filter, relative to unfiltered subsamples that were collected as described above after settling briefly (Fig. 2). This filtration-dependent DIC increase was only significant for low-DIC samples (controls and t=0), but as a precaution against this apparent gas exchange with the atmosphere during filtration, we chose to subsample for DIC without GF/F filtration.

To measure peroxides in this study, the fluorometric *p*-hydroxyphenyl acetic acid (POHPAA) dimerization method of Miller and Kester (1988), which does not distinguish between hydrogen and short-chain organic hydroperoxides, was adapted for use with a microplate reader (Fluostar, BMG). Details of this method have been published elsewhere (Miller and Kester, 1988; Miller et al., 2005). Reagents and standards here were prepared according to these previously published methods and adjusted, where necessary, to expected peroxide concentrations of 0–10 μM. H₂O₂ standards were made up in fresh artificial seawater to ensure matching refractive index of the analyte. One 96-well microplate was used per experimental suspension, each containing one set of blanks and standards and 6 sets of standard additions to samples.

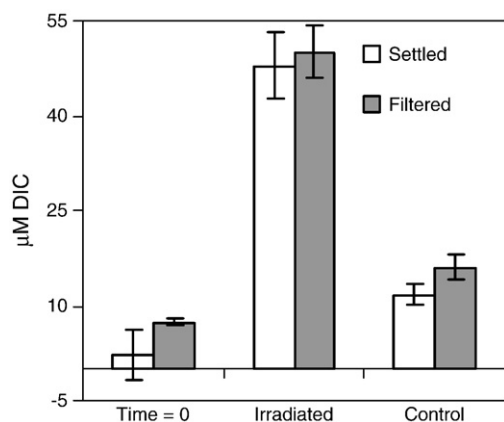


Fig. 2. DIC measured after subsampling initial, control, and irradiated suspensions allowed to settle for several minutes (white bars) or filtered through GF/F filters (gray bars). Error bars show one standard deviation (N = 3 or 4 for each bar).

After irradiation, peroxide samples were pipetted from just below the air–water interface into microplates with pre-delivered fluorometric reagent. Preliminary tests showed no effect of particulates on measured peroxide concentrations if suspensions settled briefly before subsampling. Treated samples were analyzed for POHPAA fluorescence after 30 min of reaction (Miller and Kester, 1988). Peroxide concentrations were determined by linear regression of averaged standard additions for each sample. The peroxide detection limit of this method was 0.13 μM.

Total iron was determined in the dissolved (GF/F filtrate) and ~0.7 (GF/F)–8.0 μm size fractions of sediment suspensions using colorimetric detection of the ferrozine-iron complex (Stookey, 1970; Gibbs, 1979). Irradiations were conducted in precombusted glassware as described above. Polyethylene syringes and filter holders were cleaned by 24 h in RBS detergent (Fisher Scientific) to remove organics, 48 h in 10% hydrochloric acid, and finally thorough rinsing with Milli-Q water. All other equipment for Fe analysis was cleaned as above, omitting the RBS-detergent step.

After irradiation, each suspension was filtered first through an 8.0 μm cellulose membrane filter (MF-Millipore) and the filtrate split into a 10% HCl-soaked polyethylene vial and a combusted glass beaker. Subsamples for <8.0 μm organic carbon were collected from the beaker and analyzed by the same method used for DOC determination (above). Subsamples for <8.0 μm Fe were transferred from the vial into polycarbonate cuvettes containing the acidified hydroxylamine reagent, giving a diluted concentration of 0.1 M NH₂OH in 0.1 N HCl. Remaining <8.0 μm filtrates were subsequently passed through pre-combusted GF/F filters into another vial/beaker set. These GF/F filtrates were analyzed for Fe and OC in the same way as the <8.0 μm filtrates.

Hydroxylamine-treated Fe samples were allowed to stand 40 min at room temperature, and then treated with acetate-buffered ferrozine reagent to give a diluted concentration of 0.2 mM ferrozine at pH 4.5. Sample absorbance at 562 nm was measured within 10 min of ferrozine addition, and total Fe determined against ferric chloride standards in artificial seawater. The iron detection limit using this method was 0.25 μM. Corrections for DOC light absorption in ferrozine-treated filtrates at 562 nm were not performed, because they are typically negligible (Estapa, unpub. data). Organic interference in absorption was also unlikely in the 0.7–8.0 μm fraction because there was no detectable DOC in this size range (see Results). Viollier et al. (2000) have previously shown that DOC interference in Fe-ferrozine complexation is negligible in porewaters and Suwanee River NOM with DOC concentrations an order of magnitude larger than in this study, so we assume that all iron reduced and dissolved during the reduction/acidification step was detected as the ferrozine complex.

3. Results

3.1. POC and DOC

Sediment samples irradiated for 18- to 24-hour periods typically lost 17–28% of their starting POC (Table 1). In the time series experiment, net DOC photoproduction (hereafter termed “DOC photoproduction”, as DOC loss was not measured) proceeded rapidly over the first 6-hour sampling interval, but later leveled off (Fig. 3). POC loss mirrored DOC gain although precision was not sufficient to determine reaction order for either OC pool (Fig. 3). Irradiated 1600 μM-POC algal membrane suspensions lost 21–43% of initial POC in batch experiments (Table 1). Higher-POC algal membrane suspensions (3200 μM) lost 8 and 16% of initial POC, probably due to oxygen limitation (see Oxygen section below). Corresponding dark controls in all experiments stayed the same or occasionally showed a slight increase in POC concentration (data not tabulated, a typical example is shown in Fig. 3). All photodissolution extents are consistent with

Table 1
Summary of POC irradiation experiments.

Experiment	Irradiation length (h)	Initial POC (μM)	POC lost (μM)	DOC gained (μM)	DIC gained (μM) (dark controls) ^a	O ₂ lost (μM)
FWB-500 ^b	4	834	-42			-15.8
FWB-500 ^b	24	853	-216			-67.1
FWB-500 ^b	24	841	-237	148.4		-67.3
FWB-500 ^b	18	830	-149	94.6	44.0 (13.4)	
FWB-500 ^b	19	850	-145	115.4	42.5 (12.8)	
FWB-500 ^b	22	785	-141	120.1	61.2 (15.0)	
FWB-500 ^b	24	800	-160	91.4		-80
TET-100 ^{c,d}	24	3409	-283			-202.1
TET-100 ^{c,d}	24	3167	-492			-217.7
TET-50 ^e	24	1594	-688			-178.9
TET-50 ^e	24	1650	-611	472.2		-176.4
TET-50 ^e	24	2064	-373	343.0	23.0	
TET-50 ^e	24	2064	-585	311.0	24.0	
TET-50 ^e	18	1857	-381	291.5	27.9	

^a DIC production measured in FWB dark controls was non-negligible and is given in parentheses. See text for discussion.

^b FWB-500 = Sediments from Freshwater Bayou, Louisiana resuspended at a concentration of 500 mg L⁻¹.

^c TET-100 = *Tetraselmis* sp. membrane material, resuspended at 100 mg L⁻¹.

^d Data from 100 mg L⁻¹ *Tetraselmis* membrane suspensions were not included in elemental ratios or rate calculations due to probable oxygen limitation (see text).

^e TET-50 = *Tetraselmis* sp. membrane material, resuspended at 50 mg L⁻¹.

irradiations of similar material conducted by Mayer et al. (2006, 2009a,b) under the same conditions.

3.2. Oxygen

Oxygen consumption during irradiation of both algal and sediment POC occurred at a molar ratio of 0.28 O₂ consumed to 1 POC lost (Fig. 4). Exceptions were observed in two experiments conducted using 100 mg L⁻¹ initial algal membrane concentrations (~3200 μM POC, Table 1). After 24 h of irradiation, these suspensions contained no detectable dissolved oxygen, and photodissolution extent, relative to initial POC, was less than expected (Fig. 4, open squares). Because photodissolution of algal detritus is inhibited under anoxic conditions (Mayer et al., 2009b), we inferred that the 3200 μM -OC algal detritus suspensions were oxygen-limited and hence did not include them in the $\Delta\text{POC}:\Delta\text{O}_2$ regression or other comparisons to be developed below. Although the 1600 μM -POC algal suspensions were suboxic by the end of the 24-hour irradiation experiments, they consumed

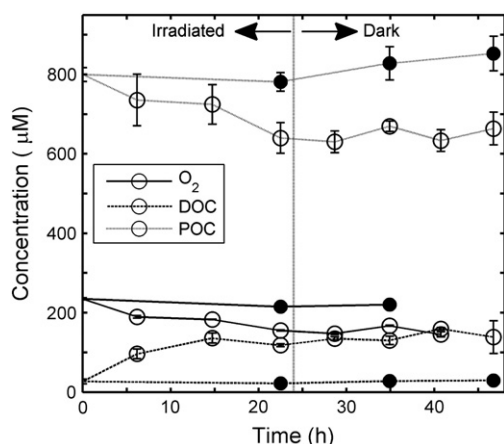


Fig. 3. Irradiation time series experiment with 500 mg-sediment L⁻¹ suspension of Freshwater Bayou sediments. Irradiation was conducted for 24 h, followed by a 24 h monitoring period in the dark. Vertical dotted black line shows the end of irradiation. Dashed lines represent non-irradiated controls, while solid lines represent irradiated suspension.

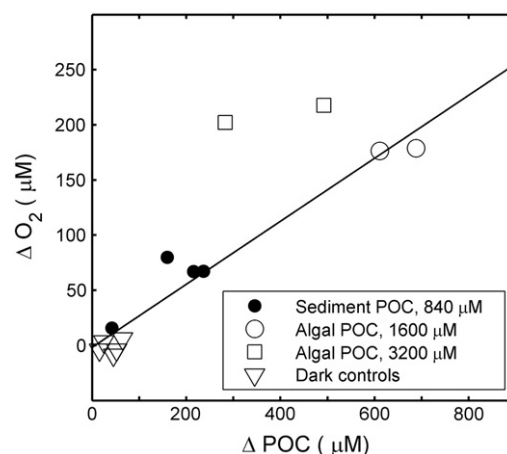


Fig. 4. Relationship between O₂ consumption and POC loss during photodissolution of Freshwater Bayou sediments and *Tetraselmis* membrane suspensions. Linear fit is through all irradiated suspensions that were not oxygen-limited (open and filled circles) and their corresponding dark controls (inverted triangles). Intercept of fit line is not significantly different from zero. Oxygen-limitation occurred in 100 mg L⁻¹ *Tetraselmis* suspensions (open squares), as discussed in text. Fit: O₂ = 0.28 * POC + 1.82. R² = 0.94, N = 12 (6 irradiated, 6 dark).

oxygen at a similar ratio to POC as in the sediment samples (Fig. 4). They also exhibited photodissolution extents similar to algal POC suspensions left open to the atmosphere, as reported in Mayer et al. (2009b). Therefore, we inferred that the 1600 μM -POC algal suspensions were not oxygen-limited. Oxygen levels were unchanged over 24 h in dark controls (Fig. 4).

3.3. DIC

DIC was produced during irradiation of both suspended sediment and algal membranes. DIC release from sediments over the irradiation periods was equivalent to 5–8% of initial POC, while algal membranes yielded only about 1–2% of initial POC (Fig. 5; see Table 1 for raw data). In non-irradiated controls, there was no DIC release from algal membrane suspensions, and a small release in sediment suspensions equivalent to 1.5–2% of initial POC. There was no significant difference in DIC concentration between replicate samples analyzed immediately after the end of an irradiation, and several hours afterward (typically 3–5 h were required to analyze all DIC samples from a single

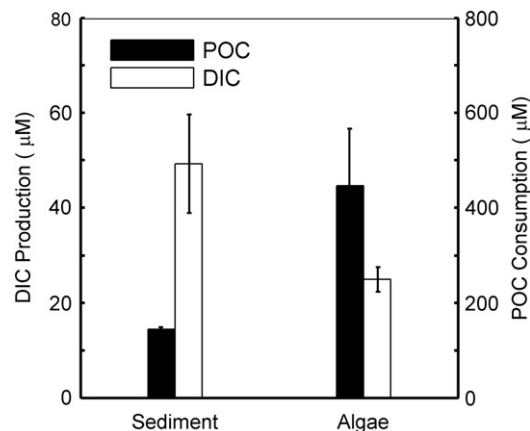


Fig. 5. Relationship between DIC production and POC loss during photodissolution of Freshwater Bayou sediments and *Tetraselmis* membrane suspensions. Relative to photodissolution of POC, *Tetraselmis* detritus suspensions underwent less photoremineralization than did Freshwater Bayou sediments.

experiment). DIC production was 37–51% of the DOC production from irradiated sediments, and 7–10% of DOC production from irradiated algal detritus.

3.4. Peroxide

In irradiated sediment suspensions, peroxide concentration rapidly increased over 2 h from an initial concentration of $0.14 \mu\text{M}$ to an apparent steady-state concentration of about $0.8 \mu\text{M}$ for the remainder of the 24 h irradiation (Fig. 6). During a subsequent 24 h in the dark, concentrations diminished with apparent second-order kinetics (Fig. 6). Peroxide concentrations in dark control sediment suspensions decreased slightly from 0.12 to $0.07 \mu\text{M}$ in the same 48 h period. Peroxide measurements reported in Mayer et al. (2009b) were conducted in irradiated suspensions of the same algal membrane material used in the present study. Their data (reanalyzed and shown in Fig. 7) will be discussed below as a point of comparison.

3.5. Iron

No significant differences were observed between total iron in the GF/F filtrate of irradiated and non-irradiated suspensions (Fig. 8, upper panel). However, in the ~ 0.7 (GF/F)– $8.0 \mu\text{m}$ fraction, total iron levels were $0.4 \mu\text{M}$ higher in the irradiated than in the non-irradiated suspensions. There was no detectable iron in artificial seawater blanks, so the iron in GF/F filtrates of both treatments, and in the 0.7 – $8.0 \mu\text{m}$ fraction of the non-irradiated treatment, presumably desorbed non-photochemically from sediments. Initially, the 500 mg L^{-1} sediment suspension contained roughly 18 – 45 mM particulate iron (based on typical 2–5% iron contents in sediments from coastal Louisiana), so the $0.4 \mu\text{M}$ enhancement in the 0.7 – $8.0 \mu\text{m}$ fraction of the irradiated suspensions represents only about 10^{-5} of the total iron in suspension. DOC photoproduction in this set of experiments was similar to other replicate experiments (Fig. 8, lower panel), and all DOC was found in the GF/F filtrate, within error.

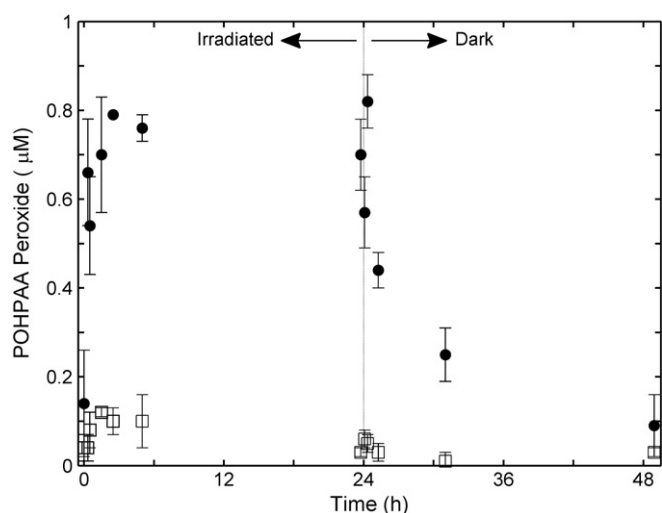


Fig. 6. Production of peroxide (using POHPAA method) during irradiation of $500 \text{ mg-sediment L}^{-1}$ Freshwater Bayou sediments. Experimental conditions were as shown in Fig. 1, with a 24-hour irradiation period followed by a 24-hour observation period in the dark. Vertical dotted line shows the end of the irradiation. Non-irradiated control is shown as a dashed line, while irradiated suspension is shown as a solid line. Peroxide concentration rapidly reached a steady-state concentration of $0.8 \mu\text{M}$, which took 24 h post-irradiation to decay back to $t=0$ levels.

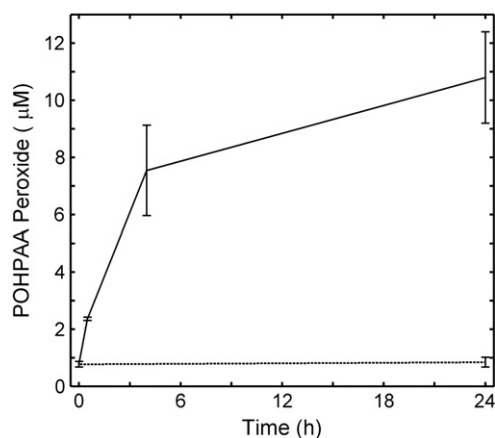


Fig. 7. Production of peroxide (using POHPAA method) during irradiation of 100 mg L^{-1} *Tetraselmis* membrane. Experimental conditions were as described in Mayer et al. (2009a,b), with a 24-hour irradiation period under open atmosphere. A non-irradiated control sample was taken at 24 h, while irradiated suspension was sampled at 0.5, 4, and 24 h. Peroxide concentration gradually increased by over an order of magnitude and had not reached steady-state by the end of the 24-hour irradiation.

4. Discussion

4.1. Abiotic vs biological DIC production

Non-irradiated control suspensions of algal membrane POC did not exhibit DIC changes over the 24-hour incubation, so DIC production in these irradiated treatments may be attributed to abiotic, photochemical remineralization. Non-irradiated control suspensions of

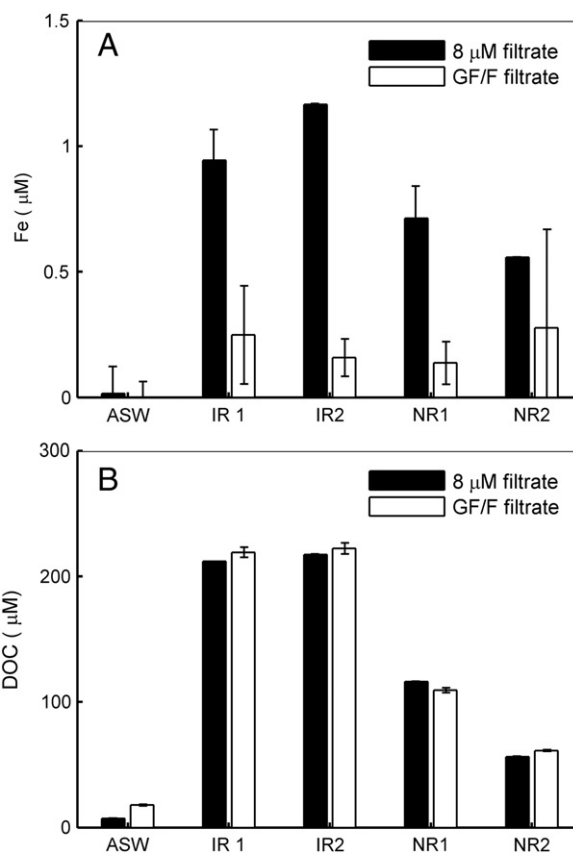


Fig. 8. Dissolved organic carbon and total iron after 24-hour treatments in GF/F and $8.0 \mu\text{m}$ filtrates of irradiated and non-irradiated sediment suspensions. ASW = artificial seawater, no sediments. IR# = irradiated suspension. NR# = dark control suspension. Upper panel (A) shows total Fe, lower panel (B) shows DOC.

sediments did release small amounts of DIC to solution (13–15 μM , Table 1). These sediments contained 0.23 mg-PIC g-sediment⁻¹ before treatment, or about 9.6 μM -PIC in each 500 mg L⁻¹ sediment suspension. The artificial seawater was made without bicarbonate and at approximately neutral pH, so initially the sediment suspensions would have been undersaturated with respect to CaCO₃. However, we cannot estimate the rate of carbonate dissolution without knowing the specific surface area of reactive carbonate minerals in the sediments (Morse et al., 2007). In the non-irradiated suspension, bacterial respiration could produce DIC. Oxygen consumption in dark sediment suspensions was not observed, but the precision of the measurements (5 μM) does not allow ruling out aerobic bacterial respiration. Anaerobic oxidation of organic matter may have also resulted in DIC production but must have been confined to anaerobic microzones within particle aggregates, as the bulk suspensions were air-saturated.

In the irradiated sediment suspensions, our data do not allow us to directly quantify the relative contributions of PIC dissolution, respiration, and photoremineralization to the observed DIC release (43–61 μM). We assume similar extents of PIC dissolution in irradiated and non-irradiation conditions, but these could range from a negligible amount (if dissolution is kinetically-limited) to a maximum of the 9.6 μM initially present as PIC. Further, dark microbial respiration may not serve as a proper control for respiration in irradiated suspensions. Ultraviolet light can inhibit bacterial activity (Herndl et al., 1993), even in Gulf of Mexico bacterial populations (Jeffrey et al., 1996). While reports show robust post-irradiation, dark recovery of bacterial metabolism, probably aided by the photoproduction of labile DOC substrates (Muller-Niklas et al., 1995; Kaiser and Herndl, 1997), our experiments had no dark recovery periods. In the following discussion, we will therefore refer to uncorrected DIC photoproduction data for sediment suspensions but, when relevant, note the effect of subtracting the dark control DIC production. The former provides an upper bound on DIC photoproduction in which kinetically-limited PIC dissolution and UV-inhibited microbial respiration are assumed, while the latter should be considered a lower limit.

4.2. Redox stoichiometries during photodissolution

Photochemical reactions of natural organic matter depend on many factors including organic carbon concentration, absorption coefficient, dosage and spectral distribution of light, and temperature. To quantify the rate of a photochemical reaction in the environment, its apparent quantum yield (AQY: the reaction rate normalized to the light absorption rate of the sample) must be determined. The absorption coefficient of natural organic matter (whether particulate or dissolved) is a complex function of composition, as well as particle size and aggregation state in the case of particles (Stramski et al., 2007; Boss et al., 2009). Consideration of the absorption spectra of our samples, a topic outside the focus of this paper, should accompany the determination of AQY values. Since the goal of this study was to survey photodissolution-related redox reactions, and compare them to the spectrum of known DOC photochemical reactions, we use a simpler alternative to absorption coefficient-normalized reaction efficiencies.

Molar ratios of the changes in concentrations of reactants and products permit us to consider net redox transformations independently of light absorption. For example, ΔDIC and ΔDOC are the changes in DIC and DOC concentrations during irradiation, averaged over all replicate experiments. The ratio $\Delta\text{DIC}:\Delta\text{DOC}$ thus expresses the net production of DIC relative to DOC after irradiation of a particular sample type, which allows comparisons among experiments with varying or unknown photochemical rate-determining conditions. We assume pseudo-first order kinetics for all carbon and oxygen pools analyzed in this way, so that the $\Delta\text{DIC}:\Delta\text{DOC}$ ratio is

independent of time (molar difference ratios were not calculated for peroxide and iron here because our measurements and numerous literature reports suggest more complicated kinetics).

Examination of the oxygen-to-carbon stoichiometries during algal membrane and sediment photodissolution shows that oxygen is consumed, and POC photodissolves, with similar ratios regardless of particle type. On the other hand, photoremineralization of POC to DIC, as measured against concurrent changes in DOC, POC, and O₂, is apparently quite sensitive to differences between POC samples. Sediments and algal detritus show similar $\Delta\text{O}_2:\Delta\text{DOC}$ and $\Delta\text{O}_2:\Delta\text{POC}$ ratios but differ in the proportion of photooxidation to photodissolution ($\Delta\text{DIC}:\Delta\text{DOC}$, $\Delta\text{DIC}:\Delta\text{POC}$) and in the amount of O₂ consumed relative to DIC produced (Fig. 9). In irradiated suspensions of sedimentary POC, net DIC production can account for up to about half of the net oxygen consumption. In algal membrane suspensions, on the other hand, DIC production can only account for, at a maximum, about 1/8th of O₂ consumption (Fig. 5).

A number of studies reported simultaneously-determined DIC photoproduction and O₂ photoconsumption rates for marine and aquatic DOC (Amon and Benner, 1996; Andrews et al., 2000; Gao and Zepp, 1998; Lindell et al., 2000; Miles and Brezonik, 1981; Xie et al., 2004). For these studies, we calculated the molar ratio of DIC production to O₂ consumption ($\Delta\text{O}_2:\Delta\text{DIC}$) during DOC photooxidation (Table 2). These DOC photooxidation data were collected from studies covering broad ranges of pH, salinity, and absorption coefficients, in which reaction rates were integrated over time periods ranging from a few hours to a day. The $\Delta\text{O}_2:\Delta\text{DIC}$ metric seems indeed to be insensitive to these variations—values for DOC photooxidation cluster at about -1:1 (i.e., 1 mol O₂ consumed per mole DIC produced). Our $\Delta\text{O}_2:\Delta\text{DIC}$ ratio of -8:1 for the algal membrane suspensions is far higher than these values, while our ratio of -1.3:1 (-1.8:1 if dark DIC production is subtracted) for the sediment suspensions is close (Table 2).

The net consumption of O₂ observed in our experiments exceeded that necessary to produce the observed DIC. While our methods didn't allow us to directly observe the "photooxygenation" (here defined as oxygen addition without complete remineralization) of organic carbon, this process is a simple explanation for otherwise unaccounted O₂ uptake. Cory et al. (2010) directly demonstrated incorporation of oxygen into fulvic acid during irradiation in the presence of ¹⁸O₂. In the present study, the observed irreversible photodissolution of OC from particles (Fig. 3) is consistent with photooxygenation-driven solubility, because oxygen-containing functional groups generally increase polarity and therefore water solubility of organic molecules (Emerson and Hedges, 2008). Irreversible photodissolution is also consistent with a simple decrease in molecular weight of organic

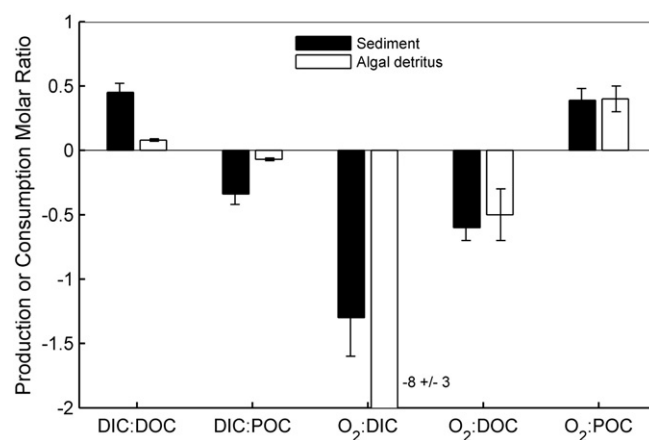


Fig. 9. Molar ratios of production/consumption of measured carbon- and oxygen-containing products and reactants during photodissolution of Louisiana sediments and algal membrane detritus suspensions. Error bars represent \pm one standard deviation.

Table 2
Summary of $\Delta\text{O}_2:\Delta\text{DIC}$ ratios in DOC literature and present study.

Publication	Site (experiment)	Description	$-\text{O}_2:\text{DIC}$ ratio (SD)
Xie et al., 2004	Satilla R.	Blackwater, high-DOM, low-pH subtropical river (24 h air-saturated treatment)	-0.74
Lindell et al., 2000	Lake Fiolen	Clear water, high latitude lake	-0.86
Lindell et al., 2000	Lake Skarshultsjon	Humic, high latitude lake	-0.86
Xie et al., 2004	Altamaha R	Whitewater, low-DOM, high-pH subtropical river (24 h air-saturated treatment)	-0.88
Amon and Benner, 1996	Rio Negro (1)	Blackwater, tropical river, 4 h irradiation	-0.88
Amon and Benner, 1996	Rio Negro (2)	See above, but 10 h irradiation	-0.88
Amon and Benner, 1996	Rio Solimoes	Sediment-laden, whitewater, tropical river (filtered)	-0.89
Amon and Benner, 1996	Rio Negro (3)	See above, but 27 h irradiation over 3 days	-0.90
Gao and Zepp, 1998	Satilla R.	0.2 μm filtered (see river description for Xie et al., above)	-1.09
Andrews et al., 2000	Various sources	$-\text{O}_2$ AQY from multiple coastal ocean sites and Shark River (subtropical blackwater), CO_2 AQY from literature	-1.1
Suspended sediments	Coastal Louisiana	This study, no subtraction of dark control DIC from irradiated DIC	-1.3 (0.3)
Suspended sediments	Coastal Louisiana	This study, subtraction of dark DIC from irradiated DIC	-1.8 (0.3)
Miles and Brezonik, 1981	Lake Mize	Highly colored subtropical lake	-2.00
Algal membrane fraction	Tetrasmis	This study	-7.69 (3)

matter (Lou and Xie, 2006) which could increase water-solubility independently of oxygen uptake.

Differences in source, and thus composition, of POC samples investigated could be related to observed differences in their photooxygenation extents. Mayer et al. (2009a) observed lignin degradation and loss from suspensions of the same sediment upon irradiation, so perhaps lignin-associated aromaticity contributed to oxygen-independent DIC photoproduction (Mopper and Kieber, 2002) in sediment suspensions, which could not occur in algal membrane suspensions. Another possible source of enhanced aromaticity in sediment POC is black carbon (Middelburg et al., 1999). Chlorophyll concentrations were 10^3 higher in algal membrane POC than in sediment POC, so photooxygenation driven by excited chlorophyll-generated reactive oxygen species (Rontani, 2001; Nelson, 1993) may have been enhanced in algal membrane suspensions. Algal-derived POC may also have been enriched in substrates likely to undergo photosensitized peroxidation, such as polyunsaturated fatty acids (Mayer et al., 2009b; Rontani, 2001).

Fig. 10 illustrates the carbon budget during sediment POC photodissolution, and potential routes for oxygen consumption. If DIC photoproduction is independent of oxygen uptake, then all oxygen must be incorporated into organic matter—either into the DOC pool alone, or by simultaneous photoaddition of oxygen to (“photooxygenation of”) both POC and DOC. If DIC photoproduction requires O_2 , then photooxygenation of organic matter must decrease accordingly. Following this logic, we can put upper and lower bounds on the stoichiometric consequences of organic matter photooxygenation by computing the organic matter O/C ratios from observations during photodissolution. For the sediment suspensions irradiated here, the total O/C ratio (summed over POC + DOC) must have increased at least by 0.02, and at most by 0.1. For algal membrane suspensions, the same total O/C ratio would increase by 0.1 regardless of whether DIC production is O_2 -independent. If all O_2 uptake is confined to algal-derived DOM, the increase could be higher (up to 0.4). Relative to the range of O/C ratios predicted for natural organic matter compound classes (Kim et al., 2003), a bulk O/C increase of 0.4 is extreme. However, algal cell membranes may be enriched in compounds with low starting O/C (e.g., lipids), while reported photoproducts such as CO, low molecular weight organic acids, and peroxides (Xie and Zafriou, 2009; Lou and Xie, 2006; CO, low molecular weight organic acids, and small organic peroxides) can have much higher O/C.

High-resolution mass spectroscopy (HRMS) has been used to investigate the redox state of carbon in analogous irradiations of DOC. Kujawinski et al. (2004) showed that irradiation of DOC led to loss of condensed (high double bond-equivalent) compounds with low

oxygen content, and preservation of more oxygen-rich, less-condensed compounds. This shift is consistent with the O/C increase suggested by our POC photodissolution data. Gonsior et al. (2009) used HRMS to examine estuarine O/DOC ratios before and after irradiation. They observed an average increase of ~ 0.1 between compounds lost from the initial sample and newly produced in the irradiated sample, although individual-compound O/C values spanned a range of about 0.5, and a negligible shift was observed when the average included unaffected compounds (supplement to Gonsior et al., 2009). These results generally suggest that DOC photooxygenation is confined to specific compounds. This possibility was directly confirmed in recent work by Cory et al. (2010) combining HRMS with labeled oxygen-uptake experiments. There, the authors showed photochemical incorporation of ^{18}O specifically into carboxyl-rich alicyclic molecules which were already present in the original sample prior to irradiation.

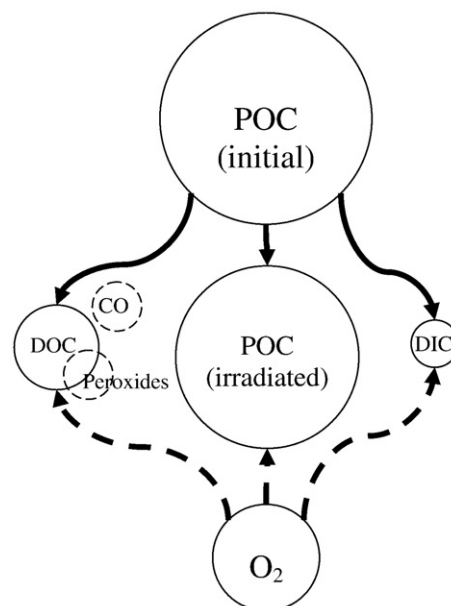


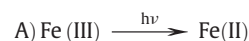
Fig. 10. Schematic showing approximate carbon budget during photodissolution of sediment POC. Areas of solid-line (POC, DOC, DIC, and O_2) circles represent relative concentrations (in carbon or dioxygen molar units) of the labeled pools. Dashed-line circles represent pools of unknown size (peroxides and CO). Solid black arrows show known carbon fluxes during photodissolution, and dashed black arrows show possible direction of unknown oxygen fluxes.

4.3. Metal and peroxide cycling

A quantitative comparison of our algal POC data to previously-reported peroxide photoproduction in algal membrane suspensions (Mayer et al., 2009b) is precluded by the higher initial POC concentrations and background peroxide concentrations in that study (Fig. 7). Nevertheless, those reported kinetics in algal membrane suspensions were quite different from those observed in the sediment suspensions in this study (Fig. 6). Although Mayer et al. (2009b) saw the peroxide concentration increase by over an order of magnitude in irradiated algal membrane suspensions, the increase was gradual and continued to the end of the 24-hour irradiation period (Fig. 7).

The low, steady-state peroxide concentrations rapidly attained in irradiated sediment suspensions (Fig. 6) are consistent with simultaneous photoproduction and photodecomposition of peroxide. The peroxide time series bears qualitative similarity to systems undergoing photo-Fenton chemistry (e.g., Fig. 4 in Southworth and Voelker, 2003) and metal-oxide photocatalyzed H₂O₂ degradation (e.g., Kormann et al., 1988). The dissimilarity between peroxide photoproduction kinetics in sediment and algal membrane suspensions suggests that the peroxide loss processes occurring in the former (possibly photo-Fenton) were absent from the latter.

The 0.4 μM increase of total iron in the 0.7–8.0 μm fraction of irradiated sediment suspensions suggests disaggregation of mineral-organic aggregates following dissolution of organic components. Alternatively, it is possible that a small fraction of the iron contained in the sediments was photoreduced and rapidly reprecipitated into this size range. Moffett and Zafriou (1993) presented evidence for Fe(II)-catalyzed, particle-associated peroxide decay in unfiltered, pH 6.5 Orinoco River water, suggesting the following reaction sequence:



They noted that if reaction “A” occurred via ligand-to-metal charge transfer, it would result in irreversible oxidation of the organic ligand, a process consistent with the organic carbon oxygenation observed here during photodissolution. Vermilyea and Voelker (2009) recently demonstrated environmentally-significant, neutral-pH, photo-Fenton chemistry in model fulvic-acid systems prepared with Fe(III) oxyhydroxides. They also used kinetic data to suggest that FeO²⁺ may play a more important role as oxidant, relative to •OH, at higher pH (Vermilyea and Voelker, 2009; Bray and Gorin, 1932). Regardless of reaction pathway, their results are consistent with heterogeneous photo-Fenton chemistry occurring in our sediment suspensions. Without information about the iron phase(s) present in the 0.7–8.0 μm particles, however, the disaggregation and Fe-photoredox cycling hypotheses are both viable. In either case, the 0.7–8.0 μm particles contain an almost negligible fraction of the total mineral iron in the suspension (27–45 mM)—not surprising given the low-Fe solubility at neutral pH conditions (Waite and Morel, 1984).

In addition to catalyzing peroxide decay, metal-oxide and natural clay and sand particles may catalyze H₂O₂ and/or hydroxyl radical formation (Gournis et al., 2002; Kormann et al., 1988; references in Waite, 1986); however, most work has focused on catalytic properties of synthetic semiconductor oxides, which make up only a small fraction of natural marine or aquatic sediments (Waite, 1986). In the present study, peroxide production rates in the first half hour of irradiation were about a factor of four higher in a 44 mg-CL⁻¹ suspension of algal POC (Fig. 7) than in a 10 mg-CL⁻¹ suspension of sediment POC (Fig. 6). The similar carbon-normalized initial peroxide

generation rates are consistent with an organic, rather than mineral, source.

4.4. Implications for turbid environments

Perhaps the most important consequence of particle-hosted photoredox reactions is the loss (and perhaps alteration) of organic carbon from the particles, which can affect organic matter accumulation in sediments. However, from a carbon-cycling perspective, introduction of DOC via photodissolution may also be important in nearshore water columns where POC comprises a significant portion of the organic carbon (e.g., hypereutrophic coastal areas adjacent to large river deltas), and absorbs a significant fraction of UV-blue light. Omission of photodissolution and associated processes from models of high-POC systems may lead to underestimates of photochemical remineralization and oxygen consumption, and ignores DOC production from and oxygen addition to non-remineralized organic matter. To quantify the magnitude of these impacts, the relative concentrations of POC and DOC and their relative absorption coefficients at UV-blue wavelengths need to be determined over the relevant spatio-temporal scales.

It remains unclear whether photoreactions and mechanisms reported in the DOC literature will apply also to POC. Published ΔO₂:ΔDIC ratios (Table 2) for DOC from a variety of aquatic and coastal environments are similar to one another and to ratios for sediment POC, suggesting qualitatively that similar photoreactive components may be involved. On the other hand, if trace metal photocycling (e.g., photo-Fenton chemistry) is involved, then the role of mineral light absorption is as relevant as that of carbon absorption. In this case, we may expect parallels between photoreactions of suspended sediments and DOC in high-Fe, freshwater systems. Differences also arise among POC samples of different origins. For instance, Xie and Zafriou (2009) observed more efficient CO production by oligotrophic POM relative to coastal POM, while we observed higher ΔDOC:ΔDIC ratios for algal-derived POM relative to sediment POM.

Any shift away from direct photoremineralization and towards production of highly-oxygenated DOC may have consequences for marine and aquatic ecosystems. In particular, some photoproducts of DOC irradiation are highly available to microbial metabolism (e.g., Miller and Moran, 1997), which leads to indirect DIC production in addition to direct photochemical DIC production (Moran and Zepp, 1997). When POC, especially fresh algal detritus, makes up a significant fraction of photochemically susceptible material in the water column, we should expect a shift in the composition of direct photoproducts away from DIC and towards photooxygenated DOC with possibly altered bioavailability. Microbial remineralization may in turn increase the indirect production of DIC, so that from the standpoint of DIC production, photochemical–microbial coupling could be enhanced in high-POC/TOC systems.

5. Conclusion

Photoreactions of marine POC include the same redox transformations that have been observed in natural DOC. Relative to DOC, the primary differences are the irreversible photodissolution of POC, and a weaker susceptibility of POC to direct photochemical remineralization. Photodissolution extents and oxygen uptake relative to photodissolution were similar for two differently-sourced POC samples, but DIC photoproduction was higher in marine sediments than algal cell membranes. The stoichiometry of oxygen consumption and carbon oxidation during photodissolution suggests oxygen incorporation into organic matter without full remineralization, increasing the O/C ratio of sediment organic carbon by 0.02–0.1 and algal organic carbon by 0.1–0.4. Peroxide kinetics and iron dynamics suggest the involvement

of photo-Fenton chemistry in photodissolution of sediment POC, but not algal POC.

These observations suggest that photodissolved organic carbon from suspended POC (produced during blooms or coastal resuspension events) is likely to be oxygenated, and that absorption of light by POC to the exclusion of DOC during such events may decrease overall direct photochemical DIC production but change the amount of indirect DIC production via microbial DOC uptake. Resuspension of sediments may also increase the importance of photo-Fenton processes in otherwise low-Fe coastal ocean water columns. Quantitative versions of these predictions will require accurate partitioning of light absorption among the photochemically-reactive materials in the water column, a question to be addressed in further work.

Acknowledgements

The authors would like to thank Kathy Thornton and Linda Schick for assistance with DOC and iron analyses. Linda Kalnejais provided helpful advice on iron determination methodologies. Funding for this work was provided by NSF Chemical Oceanography. Partial support for M.L.E. was provided by the Petroleum Research Fund and by a NASA Earth Systems Science Fellowship.

References

- Amon, R., Benner, R., 1996. Photochemical and microbial consumption of dissolved organic carbon and dissolved oxygen in the Amazon River system. *Geochim. Cosmochim. Acta* 60 (10), 1783–1792.
- Andrews, S.S., Zafriou, O.C., Caron, S., 2000. Photochemical oxygen consumption in marine waters: a major sink for colored dissolved organic matter? *Limnol. Oceanogr.* 45 (2), 267–277.
- Blough, N.V., Zepp, R.G., 1995. Reactive oxygen species in natural waters. In: Foote, C.S., Valentine, J.S., Liebman, J.F. (Eds.), *Active Oxygen in Chemistry*. Chapman & Hall, USA.
- Boss, E., Slade, W., Hill, P., 2009. Effect of particulate aggregation in aquatic environments on the beam attenuation and its utility as a proxy for particulate mass. *Opt. Express* 17 (11), 9408–9420.
- Bray, W.C., Gorin, M.H., 1932. Ferryl ion, a compound of tetravalent iron. *J. Am. Chem. Soc.* 54 (5), 2124–2125.
- Carpenter, J.H., 1965. The Chesapeake Bay Institute technique for the Winkler dissolved oxygen method. *Limnol. Oceanogr.* 10 (1), 141–143.
- Cooper, W.J., Zika, R.G., Petasne, R.G., Plane, J.M.C., 1988. Photochemical formation of H₂O₂ in natural waters exposed to sunlight. *Environ. Sci. Technol.* 22, 1156–1160.
- Cory, R.M., McNeill, K., Cotner, J.P., Amado, A., Purcell, J.M., Marshall, A.G., 2010. Singlet oxygen in the coupled photochemical and biochemical oxidation of dissolved organic matter. *Environ. Sci. Technol.* 44 (10), 3683–3689.
- Emerson, S., Hedges, J., 2008. *Chemical Oceanography and the Marine Carbon Cycle*. Cambridge University Press, New York.
- Gao, H., Zepp, R.G., 1998. Factors influencing photoreactions of dissolved organic matter in a coastal river of the southeastern United States. *Environ. Sci. Technol.* 32 (19), 2940–2946.
- Gibbs, M., 1979. A simple method for the rapid determination of iron in natural waters. *Water Res.* 13, 295–297.
- Gonsior, M., Peake, B.M., Cooper, W.T., Podgorski, D., D'Andrilli, J., Cooper, W.J., 2009. Photochemically induced changes in dissolved organic matter identified by ultrahigh resolution Fourier transform ion cyclotron resonance mass spectrometry. *Environ. Sci. Technol.* 43 (3), 698–703.
- Gourmis, D., Karakassides, M.A., Petridis, D., 2002. Formation of hydroxyl radicals catalyzed by clay surfaces. *Phys. Chem. Miner.* 29 (2), 155–158.
- Herndl, G.J., Muller-Niklas, G., Frick, J., 1993. Major role of ultraviolet-B in controlling bacterioplankton growth in the surface layer of the ocean. *Nature* 361, 717–719.
- Horowitz, A.J., Elrick, K.A., Smith, J.J., 2001. Annual suspended sediment and trace element fluxes in the Mississippi, Columbia, Colorado, and Rio Grande drainage basins. *Hydrol. Process.* 15 (7), 1169–1207.
- Jeffrey, W., Pledger, R., Aas, P., Hager, S., Coffin, R., Von Haven, R., Mitchell, D., 1996. Diel and depth profiles of DNA photodamage in bacterioplankton exposed to ambient solar ultraviolet radiation. *Mar. Ecol. Prog. Ser.* 137, 283–291.
- Kaiser, E., Herndl, G.J., 1997. Rapid recovery of marine bacterioplankton activity after inhibition by UV radiation in coastal waters. *Appl. Environ. Microbiol.* 63 (10), 4026–4031.
- Kieber, R.J., Whitehead, R.F., Skrabal, S.A., 2006. Photochemical production of dissolved organic carbon from resuspended sediments. *Limnol. Oceanogr.* 51 (5), 2187–2195.
- Kim, S., Kramer, R.W., Hatcher, P.G., 2003. Graphical method for analysis of ultrahigh-resolution broadband mass spectra of natural organic matter, the van Krevelen diagram. *Anal. Chem.* 75, 5336–5344.
- Kormann, C., Bahnemann, D.W., Hoffman, M.R., 1988. Photocatalytic production of H₂O₂ and organic peroxides in aqueous suspensions of TiO₂, ZnO, and desert sand. *Environ. Sci. Technol.* 22, 798–806.
- Kujawinski, E.B., Del Vecchio, R., Blough, N.V., Klein, G., Marshall, A.G., 2004. Probing molecular-level transformations of dissolved organic matter: insights on photochemical degradation and protozoan modification of DOM from electrospray ionization Fourier transform ion cyclotron resonance mass spectrometry. *Mar. Chem.* 92, 23–37.
- Lindell, M., Graneli, H., Bertilsson, S., 2000. Seasonal photoreactivity of dissolved organic matter from lakes with contrasting humic content. *Can. J. Fish. Aquat. Sci.* 57 (5), 875–885.
- Lou, T., Xie, H., 2006. Photochemical alteration of the molecular weight of dissolved organic matter. *Chemosphere* 65, 2333–2342.
- Mayer, L.M., 1994. Surface area control of organic carbon accumulation in continental shelf sediments. *Geochim. Cosmochim. Acta* 58, 1271–1284.
- Mayer, L.M., Schick, L.L., Skorko, K., Boss, E., 2006. Photodissolution of particulate organic matter from sediments. *Limnol. Oceanogr.* 51 (2), 1064–1071.
- Mayer, L.M., Schick, L.L., Bianchi, T.S., Wysocki, L.A., 2009a. Photochemical changes in chemical markers of sedimentary organic matter source and age. *Mar. Chem.* 113 (1–2), 123–128.
- Mayer, L.M., Schick, L.L., Hardy, K.R., Estapa, M.L., 2009b. Photodissolution and other photochemical changes upon irradiation of algal detritus. *Limnol. Oceanogr.* 54 (5), 1688–1698.
- Middelburg, J.J., Nieuwenhuize, J., van Breugel, P., 1999. Black carbon in marine sediments. *Mar. Chem.* 65 (3–4), 245–252.
- Miles, C.J., Brezonik, P.L., 1981. Oxygen consumption in humic-colored waters by a photochemical ferrous-ferric catalytic cycle. *Environ. Sci. Technol.* 15 (9), 1089–1095.
- Miller, W.L., Kester, D., 1988. Hydrogen peroxide measurement in seawater by (p-hydroxyphenyl)acetic acid dimerization. *Anal. Chem.* 60, 2711–2715.
- Miller, W.L., Moran, M.A., 1997. Interaction of photochemical and microbial processes in the degradation of refractory dissolved organic matter from a coastal marine environment. *Limnol. Oceanogr.* 42 (6), 1317–1324.
- Miller, W.L., Zepp, R.G., 1995. Photochemical production of dissolved inorganic carbon from terrestrial organic matter: significance to the oceanic organic carbon cycle. *Geophys. Res. Lett.* 22 (4), 417–420.
- Miller, W.L., King, D.W., Lin, J., Kester, D.R., 1995. Photochemical redox cycling of iron in coastal seawater. *Mar. Chem.* 50 (1–4), 63–77.
- Miller, G.W., Morgan, C.A., Kieber, D.J., King, D.W., Snow, J.A., Heikes, B.G., Mopper, K., Kiddle, J.J., 2005. Hydrogen peroxide method intercomparison study in seawater. *Mar. Chem.* 97, 4–13.
- Moffett, J.W., Zafriou, O.C., 1993. The photochemical decomposition of hydrogen peroxide in surface waters of the eastern Caribbean and Orinoco River. *J. Geophys. Res.* 98 (C2), 2307–2313.
- Mopper, K., Kieber, D.J., 2002. Photochemistry and the cycling of carbon, sulfur, nitrogen, and phosphorus. In: Hansell, D.A., Carlson, C.A. (Eds.), *Biogeochemistry of Marine Dissolved Organic Matter*. Academic Press, USA, pp. 455–508.
- Moran, M.A., Zepp, R.G., 1997. Role of photoreactions in the formation of biologically labile compounds from dissolved organic matter. *Limnol. Oceanogr.* 42 (6), 1307–1316.
- Morse, J.W., Arvidson, R.S., Luttge, A., 2007. Calcium carbonate formation and dissolution. *Chem. Rev.* 107, 342–381.
- Muller-Niklas, G., Heissenberger, A., Puskaric, S., Herndl, G.J., 1995. Ultraviolet-B radiation and bacterial metabolism in coastal waters. *Aquat. Microb. Ecol.* 9, 111–116.
- Nelson, J.R., 1993. Rates and possible mechanism of light-dependent degradation of pigments in detritus derived from phytoplankton. *J. Mar. Res.* 51, 155–179.
- Obernosterer, I., Ruardij, P., Herndl, G.J., 2001. Spatial and diurnal dynamics of dissolved organic matter (DOM) fluorescence and H₂O₂ and the photochemical oxygen demand of surface water DOM across the subtropical Atlantic Ocean. *Limnol. Oceanogr.* 46 (3), 632–643.
- O'Sullivan, D.W., Neale, P.J., Coffin, R.B., Boyd, T.J., Osburn, C.L., 2005. Photochemical production of hydrogen peroxide and methylhydroperoxide in coastal waters. *Mar. Chem.* 97 (1–2), 14–33.
- Perez Jr., B.C., J.W.D., Rouse, L.J., Shaw, R.F., Wang, M., 2000. Influence of Atchafalaya River discharge and winter frontal passage on suspended sediment concentration and flux in Fourleague Bay, Louisiana. *Estuarine, Coastal and Shelf Science* 50, 271–290.
- Riggsbee, J., Orr, C., Leech, D., Doyle, M., Wetzel, R., 2008. Suspended sediments in river ecosystems: photochemical sources of dissolved organic carbon, dissolved organic nitrogen, and adsorptive removal of dissolved iron. *J. Geophys. Res.* 113 (G03019).
- Rontani, J., 2001. Visible light-dependent degradation of lipidic phytoplanktonic components during senescence: a review. *Phytochemistry* 58 (2), 187–202.
- Southworth, B.A., Voelker, B.M., 2003. Hydroxyl radical production via the photo-Fenton reaction in the presence of fulvic acid. *Environ. Sci. Technol.* 37 (6), 1130–1136.
- Stokey, L.L., 1970. Ferrozine—a new spectrophotometric reagent for iron. *Anal. Chem.* 42 (7), 779–781.
- Stramski, D., Babin, M., Wozniak, S., 2007. Variations in the optical properties of terrigenous mineral-rich particulate matter suspended in seawater. *Limnol. Oceanogr.* 52 (6), 2418–2433.
- Swarczewski, P., Baskaran, M., Rosenbauer, R., Orem, W., 2006. Historical trace element distribution in sediments from the Mississippi River delta. *Estuaries Coasts* 29 (6), 1094–1107.
- Vermilyea, A.W., Voelker, B.M., 2009. Photo-Fenton reaction at near neutral pH. *Environ. Sci. Technol.* 43 (18), 6927–6933.
- Viollier, E., Inglett, P.W., Hunter, K., Roychoudhury, A.N., Van Cappellen, P., 2000. The ferrozine method revisited: Fe(II)/Fe(III) determination in natural waters. *Appl. Geochem.* 15 (6), 785–790.

- Waite, T.D., 1986. Photoredox chemistry on colloidal metal oxides. In: Davis, J.A., Hayes, K.F. (Eds.), *Geochemical Processes at Mineral Surfaces*. ACS Symposium Series. American Chemical Society, Chicago.
- Waite, T.D., Morel, F.M.M., 1984. Photoreductive dissolution of colloidal iron oxides in natural waters. *Environ. Sci. Technol.* 18 (11), 860–868.
- Xie, H., Zafriou, O.C., 2009. Evidence for significant photochemical production of carbon monoxide by particles in coastal and oligotrophic marine waters. *Geophys. Res. Lett.* 36 (23), L23606.
- Xie, H., Zafriou, O.C., Cai, W., Zepp, R.G., Wang, Y., 2004. Photooxidation and its effects on the carboxyl content of dissolved organic matter in two coastal rivers in the southeastern United States. *Environ. Sci. Technol.* 38 (15), 4113–4119.
- Zafriou, O.C., 2002. Sunburnt organic matter: biogeochemistry of light-altered substrates. *Limnol. Oceanogr. Bull.* 11 (4), 69–71.